Synthesis of carbon fibers arrays by the sol-gel process

Samantha L. Flores-López, Sara F. Villanueva, Miguel A. Montes-Morán, Ana Arenillas*

Instituto de Ciencia y Tecnología del Carbono, INCAR-CSIC. Francisco Pintado Fe, 26. 33011 Oviedo, Spain

* Corresponding author Email: ana.arenillas@csic.es

ABSTRACT

This study presents a new route for the synthesis of carbon gels with a structure that includes aligned fibers of the same material. A modification of the heating process during polymerization of resorcinol and formaldehyde produces a combination of the classical polymeric nodules in carbon gels with arrays of totally aligned fibers. This new morphology, produced through a very simple process, opens up new application possibilities to the already numerous existing ones for carbon gels.

Keywords: Carbon fibers arrays, Sol-gel process

1. Introduction

The inclusion of structures such as fibers, filaments and tubes into carbon materials have shown promising results for applications in energy, electronics, and purification processes [1–4]. However, the advantages that these peculiar morphologies add to the material are as wide as the complexity of their synthesis [4–6]. Taking advantage of the versatility of the sol-gel process to design and produce synthetic carbons with very well controlled properties, this study presents a new route for the synthesis of carbon gels with a structure that includes aligned fiber arrays of the same material. In addition, it evaluates the effect of different synthesis variables on the distribution and growth of these new arrays.

2. Experimental procedure

Organic gels were prepared from homogeneous mixtures of resorcinol (R) and formaldehyde (F), keeping the stoichiometric ratio (i.e., R/F 0.5). To get different dilution ratios [7] (i.e., D 5.6 and 6.5), deionized water was added as a solvent. Finally, the pH of the precursor mixtures was adjusted to 2 or 2.7 using HNO_3. Precursor solutions were placed into an oven at 85°C to start the polymerization process. The common sol-gel route was interrupted by a variation of the heating process, passing the solutions from the oven to a water-bath at 60°C and maintained there until the gelation process was complete (i.e. a solid material was obtained). Three different points of the polymerization progress were selected to make the change: early polymerization (EP), late polymerization (LP) and viscous point (VP). Where EP was identified by the presence of an oily appearance, LP by a whitish appearance, and VP by the densification of the precursor solution. Gels were then relocated into the oven at 85°C for ageing and drying steps. Finally, carbon gels were obtained from the carbonization of these organic samples at 750°C for 2 h in an inert atmosphere (i.e. flow of150 mL/min of N_2).The samples are identified as CX followed by the pH value, the dilution ratio, and the breakpoint of the sol-gel route (i.e. EP, LP or VP).

The morphology of the different structures formed was evaluated using scanning electron microscopy (SEM, Quanta FEG 650). Samples were also outgassed at 120ºC overnight to be characterized by helium pycnometry (AccuPyc 1330 from Micromeritics), N_2 adsorption-desorption isotherms at -196ºC (Tristar II from Micromeritics) and mercury porosimetry (AutoPore IV porosimeter from Micromeritics), in order to obtain pore characterization: helium densities (ρ_{He}), pore volumes (V_{Total},V_{Micro},V_{Meso},V_{Macro}) and pore size distributions (PSD). All samples, due to their morphology, showed compression at the initial stages of the mercury intrusion analysis. Therefore pore volumes and PSD were corrected using the equations developed by Job et. al. [8]. Additionally, their envelope densities (ρ_{Env}) were

calculated using the tapping test, and the porosity (P) was thus determined according to the following equation:

$$P = \left(1 - \frac{\rho_{Env}}{\rho_{He}}\right) \times 100 \quad (1)$$

3. Results and discussion

Modification of the temperature and heating method used during the polymerization process results in morphological variations of carbon gels. Figure 1a shows how this variation produces a change from typical carbon gel structures (i.e. interconnected polymeric nodules) to a direct formation of fibers within the same precursor mixture, resulting in materials with novel hybrid morphologies (i.e. combinations of polymeric nodules and aligned fibers of the same composition). Both, the monolith (inset in Fig.1a) and SEM images of CX-2.7-5.6-EP samples how a low-density material formed by a combination of semi-fused node networks and aligned fibers. In this sample, these fibers exhibit different lengths and some seem to be still incomplete. In contrast, the sample obtained by a change of the heating process to the most advanced polymerization point (i.e., CX-2.7-5.6-VP) shows considerable densification, as can be seen in the inset image of the monolith, and a very different morphology observed by SEM, with a layered arrangement and no fibers at all. However, sample CX-2.7-5.6-LP, with a modification of the heating process to an intermediate stage, also presents intermediate density. In this case, it is worth noting that the formation of aligned fibers seems to be favored, and hybrid structures can be very clearly seen in Fig. 1a. The length of these fibers is such that they can be observed even without magnification, making LP the most suitable point for obtaining this kind of morphology. In agreement with these observations, Table 1 shows how starting from a more advanced polymerization stage results in samples with higher density (ρ_{Env}), lower porosity (P), and lower total pore volume (V_{Total}). In addition, the PSD in Figure 1b shows a decreasing trend in the characteristic pore size for samples

EP>LP>VP. Moreover, sample CX-2.7-5.6-VP also shows a considerable increase of narrow pores around 10 nm.

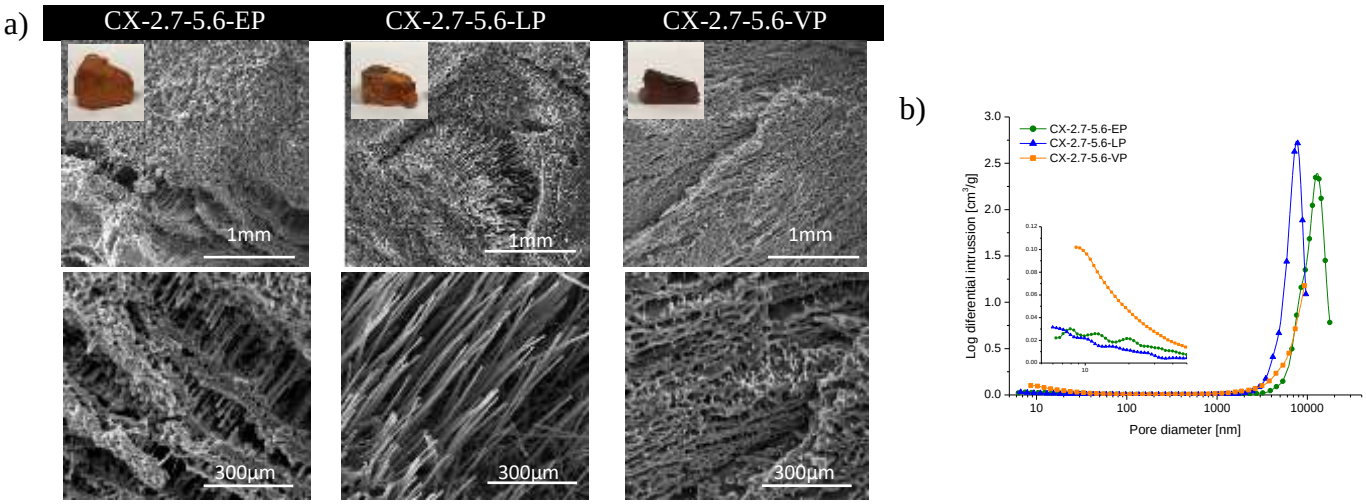

Figure 1. Influence on aligned fiber formation with the change of heating process in the different polymerization stages: early polymerization (EP), late polymerization (LP) and viscous point (VP): a) SEM micrographs; b) pore size distribution obtained by mercury porosimetry.

Table 1. Porous properties of the monolithic carbon gels containing aligned fibers in this study: helium and envelope densities, porosity and pore volumes.

Sample	ρ_{He} (g/cm^3)	ρ_{Env} (g/cm^3)	P %	V_{Total} (cm^3/g)	V_{Micro} (cm^3/g)	V_{Meso} (cm^3/g)	V_{Macro} (cm^3/g)
CX-2.7-5.6-EP	1.88	0.60	68	0.89	0.22	0.02	0.66
CX-2.7-5.6-LP	1.86	0.62	67	0.84	0.23	0.02	0.60
CX-2.7-5.6-VP	1.85	0.69	63	0.44	0.23	0.04	0.17
CX-2.7-6.5-LP	1.89	0.65	66	0.78	0.26	0.01	0.51
CX-2.0-5.6-LP	1.87	0.52	72	0.99	0.21	0.01	0.78

According to the above results, the change of the heating process to the LP point seems to be the most favorable for the production of aligned fibers in the carbon structure. Therefore, Figure 2 shows the effect of other synthesis variables that are usually significant in the polymerization process of resorcinol and formaldehyde (i.e. dilution and pH of the precursor solution) at this point. SEM micrographs of sample CX-2.7-6.5-LP (see Figure 2a) show that the effect of increasing the dilution ratio is very similar to the effect seen in traditional RF gels. The resultant materials exhibit larger pore spaces [7, 9], and the fibers seem to be thicker and formed in lower numbers. Therefore, increasing dilution does not favor the formation of aligned fibers. On the other hand, when acid catalysis is used during RF

polymerization, it is expected that greater amounts of catalyst (i.e., lower pH) favor the initiation reaction and therefore the formation of more small-sized clusters will be promoted [10]. In the same way, sample CX-2.0-5.6-LP exhibits fiber formation but the fibers are well distributed throughout the sample, and smaller arrays are observed.

Although not shown in this letter, the opposite conditions for these variables were also evaluated (i.e., higher pH and lower dilution ratio), resulting in considerable densification of the materials, with no fiber formation at all.

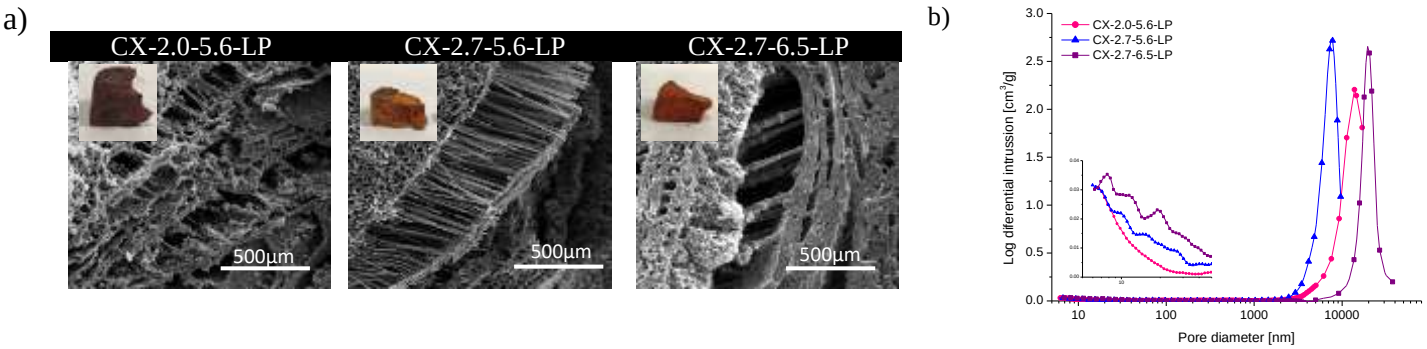

Figure 2. Effect of pH and dilution ratio (D) in the formation of aligned fibers. a) SEM images; b) pore size distribution obtained by mercury porosimetry.

All samples have similar V_{Micro} (see Table 1) corresponding to specific surface areas ca. 610 m^2/g and mainly generated during the carbonization process. In addition, all the samples produced are macroporous, since the main contribution to the total pore volume comes from macropores formed between fiber arrays.

4. Conclusions

Slight changes in the heating process during the polymerization step may have a great influence on the final morphology of RF carbon gels. In this study, small deviations from the usual synthesis route encouraged the formation of polymeric aligned fibers instead of the classical nodules. This is the first time these completely-aligned fibers have been produced directly by a sol-gel process using moderate operating conditions. The formation of these

aligned fibers is favored if the precursor mixture is allowed to polymerize at 85ºC, until just before it becomes viscous (i.e. the late polymerization point), and then the temperature is reduced to 60ºC. In addition, the dilution ratio and pH of the precursor mixture also play an important role, in a similar way as in classical RF gels. This new synthesis procedure not only leads to a carbon material with a very good combination of porosity and surface area but also a novel morphology, combining polymeric nodules and aligned fibers, produced by a single process.

Acknowledgements

The authors are grateful to the Spanish Ministerio de Economia, Industria y Competitividad (CTQ2017-87820-R) and the Principality de Asturias–FICYT-FEDER(IDI/2018/000118) for their financial support.SFL is grateful for her research training grant received from the Administración del Principado de Asturias through the "Severo Ochoa" program.

References

1. Ameli A, Jung PU, Park CB (2013) Electrical properties and electromagnetic interference shielding effectiveness of polypropylene/carbon fiber composite foams. Carbon 60:379–391. https://doi.org/10.1016/j.carbon.2013.04.050
2. Haghgoo M, Yousefi AA, Mehr MJZ, et al (2015) Correlation between morphology and electrical conductivity of dried and carbonized multi-walled carbon nanotube/ resorcinol–formaldehyde xerogel composites. Journal of Materials Science 50:6007–6020. https://doi.org/10.1007/s10853-015-9148-0
3. Burchell TD, Eatherly WP, Strizak JP (2000) Activated carbon fiber composite materials and method of making. 4
4. Hassan MF, Sabri MA, Fazal H, et al (2020) Recent trends in activated carbon fibers production from various precursors and applications—A comparative review. Journal of Analytical and Applied Pyrolysis 145:104715. https://doi.org/10.1016/j.jaap.2019.104715
5. Szczurek A, Barcikowski M, Leluk K, et al (2017) Improvement of Interaction in a Composite Structure by Using a Sol-Gel Functional Coating on Carbon Fibers. Materials 10:990. https://doi.org/10.3390/ma10090990
6. Tekinalp HL, Kunc V, Velez-Garcia GM, et al (2014) Highly oriented carbon fiber–polymer composites via additive manufacturing. Composites Science and Technology 105:144–150. https://doi.org/10.1016/j.compscitech.2014.10.009
7. Rey-Raap N, Arenillas A, Menéndez JA (2016) A visual validation of the combined effect of pH and dilution on the porosity of carbon xerogels. Microporous and Mesoporous Materials 223:89–93. https://doi.org/10.1016/j.micromeso.2015.10.044
8. Job N, Pirard R, Pirard J-P, Alié C (2006) Non Intrusive Mercury Porosimetry: Pyrolysis of Resorcinol-Formaldehyde Xerogels. Particle & Particle Systems Characterization 23:72–81. https://doi.org/10.1002/ppsc.200601011
9. Alonso-Buenaposada ID, Rey-Raap N, Calvo EG, et al (2017) Acid-based resorcinol-formaldehyde xerogels synthesized by microwave heating. Journal of Sol-Gel Science and Technology 84:60–69. https://doi.org/10.1007/s10971-017-4475-z
10. ElKhatat AM, Al-Muhtaseb SA (2011) Advances in Tailoring Resorcinol-Formaldehyde Organic and Carbon Gels. Advanced Materials 23:2887–2903. https://doi.org/10.1002/adma.201100283